

Interrelation of light backscattering and attenuation in upper layers of Lake Baikal

G.P. Kokhanenko,¹ V.G. Ivanov,² and P.P. Sherstyankin²

¹*Institute of Atmospheric Optics,
Siberian Branch of the Russian Academy of Sciences, Tomsk*
²*Limnological Institute,
Siberian Branch of the Russian Academy of Sciences, Irkutsk*

Received January 18, 2007

The relations between the indices of light attenuation and backscattering in the upper 300-meter water layer of Lake Baikal are presented. The data were obtained during measurements of the depth profiles of hydro-optical characteristics in different water areas of the Lake in March and August, 2003. The obtained relations are compared with the available results for the ocean and sea waters. A certain ambiguity of dependences for the regions with maximal (more than 1.2 m⁻¹) attenuation index is found.

Introduction

The manifold optical parameters of natural waters of seas and internal reservoirs are subjected to seasonal variability. A close proximity of large rivers, carrying great masses of mineral particles to the water reservoirs, essentially affects the interrelation between different hydro-optical characteristics. However, the main component determining the optical parameters in the regions located far from river flows is the hydrosol of biological origin, i.e., zoo- and phytoplankton developed due to the solar radiation. The relations between the optical parameters of the medium in different water reservoirs can have common regularities. The major part of Lake Baikal water area also refers to such regions.

The regularities of distribution and variability of hydro-optical characteristics in seas and oceans are generalized, for example, in Refs. 1–4. At present, the models are known, describing the interrelations between individual optical parameters, based both on the experimental data analysis and on theoretical calculations.^{5–9} The specified models are necessary, when processing the space remote sensing data on the sea surface. The development of remote sensing methods requires the amendment of well-known models for the coastal areas and internal reservoirs.

An important part of such models are relations between the attenuation and backscattering indices, necessary for interpretation of observations of spectral composition of radiation, reflected from the surface, as well as at laser sensing of the upper water layer. This paper presents data on connection between attenuation and backscattering in the upper 300-meter layer of Lake Baikal.

1. Measurements of hydro-optical characteristics

The measurements were carried out in 2003 at the end of March, from the ice cover in the region of NT200 neutrino telescope location (cape Ivanovsky in the southern part of Lake Baikal, 3.5 km from the coast) and in August from the board of the Research Vessel *G.Yu. Vereshchagin*. Both periods are characterized by the maximal phytoplankton development and the increased water turbidity in the surface layer. In total, three vertical profiles were obtained in March, and 31 profiles in August, 9–16. Figure 1 shows the location of monitoring stations.

The conventional symbols, which mark the position of stations, are determined by the type of vertical profiles of the attenuation index, which will be described further.

The main optical parameters of the scattering medium are the absorption index a and the index of the directed scattering $\beta(\gamma)$, determining the integral scattering index

$$b = 2\pi \int_0^{\pi} \beta(\gamma) \sin \gamma d\gamma$$

(γ is the scattering angle). Besides, the backscattering index

$$b_B = 2\pi \int_{\pi/2}^{\pi} \beta(\gamma) \sin \gamma d\gamma$$

and the backscattering probability $B = b_B/b$ are used, respectively, as well as the attenuation index $c = a + b$. To determine the backscattering index in the hydro-optical measurements, a simple measuring

method of measuring $\beta(\gamma)$ at fixed scattering angle γ equal to 140° is commonly used.



Fig. 1. Location of monitoring stations at Lake Baikal in 2003.

The theoretical analysis of the scattering phase function variability for different types of water¹⁰ has shown that in this case $b_B = \chi\beta_{140}$, where χ is the coefficient, determining the relation between β_{140} at $\gamma = 140^\circ$ and b_B . Reference 10 gives the χ calculated value of 6.78 at a root-mean-square error of 9%. Reference 11 gives somewhat greater value of χ (7.23) from the processing of more than 800 experimental phase functions.

For *in situ* measurements, the *c*-beta immersion device (HOBILabs, Inc.) was applied.¹² Radiation with $\lambda = 532$ nm was used in the device. The attenuation index *c* was measured on a path of 0.3 m and the scattering index β_{140} at an angle of 140° . In the course of measurements, the device was immersing down to the maximal depth *h* equal to 300 m at a constant velocity of about 0.5 m/s. The readings were taken one time per second and were compared with the simultaneous measurements conducted with the immersed photometer-transparency meter¹³ with a base of 1 m. Deviations of the measured values did not exceed 0.02 m^{-1} under 200 m. The random measurement errors of attenuation index can be estimated in Fig. 2a, where the data obtained during the device hanging at a depth of 241 m during 100 s are shown in the right bottom corner.

The data show the spread of measured values induced both by random measurement errors (including the depth sensor) and by medium fluctuations. The spread of measured values of β_{140} is shown in Fig. 2b by the points in the top of two curves. The root-mean-square deviations are $\sigma_\epsilon = 0.01 \text{ m}^{-1}$ and $\sigma_\beta = 0.0014 \text{ m}^{-1} \cdot \text{sr}^{-1}$.

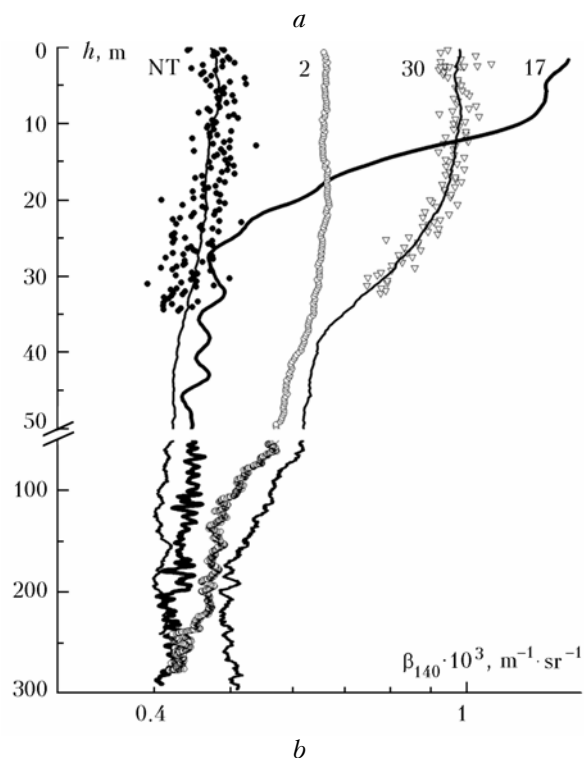
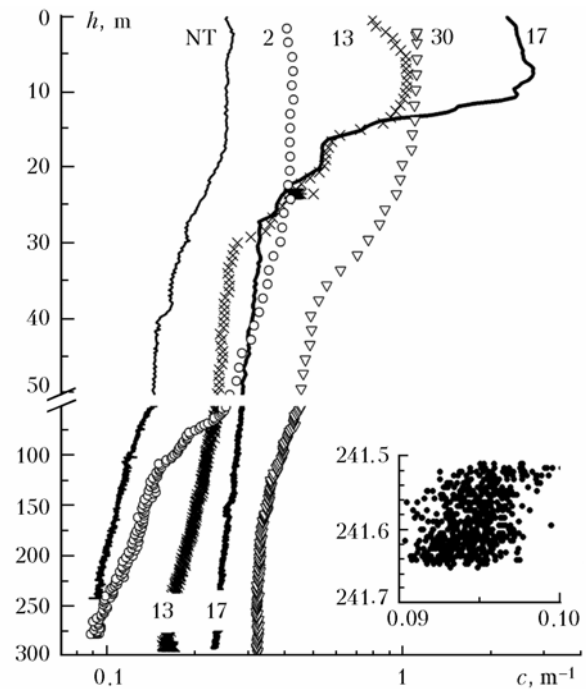


Fig. 2. The typical vertical profiles of attenuation and backscattering indices in the upper water layer.

A stable stratification, characterized by the absence of vertical mixing of the surface and deep waters, is observed in Lake Baikal. In the upper layers, after the homothermie (June and November), there appears a seasonal layer of density jump at depths between 10 and 30 m, gradually sinking deeper with water heating in spring and summer.¹⁴ The density jump prevents the free settling of hydrosol particles of organic origin. As a result, the water transparency below this level quickly increases. The examples of vertical profiles of c and β_{140} are presented in Fig. 2. The number of monitoring station is denoted by figures near curves, and the profile obtained on March 30, 2003 from ice cover is denoted by letters NT.

It is possible to distinguish two types of vertical profiles of attenuation index in the surface layer. In the first case, an approximately constant attenuation value in the near-surface layer is observed and then the attenuation decreases under the jump layer. The profiles were observed in winter and in summer (at stations located in the southern part of Lake Baikal) are referred to the first type (Fig. 1). Figure 2 presents stations 2 and 30 with minimal (0.43 m^{-1}) and maximal (1.2 m^{-1}) values of c . The second type of distribution is characterized by the well-defined maximum in the c profile at $h_{\text{max}} \approx 8\text{--}10 \text{ m}$ (type 2 in Fig. 1). The attenuation values for this type were within the limits from 1 m^{-1} (station 13) to 2.7 m^{-1} (station 17). Undoubtedly, this maximum is caused by the increased plankton concentration at these depths and is observed both at day and night time. In some cases, the maxima are possible directly above the jump layer due to sedimentation of organic particles. Such cases were observed at stations 22 and 24, and sometimes in spring in the subglacial layer.^{13,15} The region of sedimentation of mineral particles near the Selenga mouth refers to a particular type, which is not considered in this work (type 3 in Fig. 1), where the layers of strong turbidity are observed near the bottom.

Figure 2b shows the profiles of β_{140} . As a whole, the vertical behavior of β_{140} corresponds to that of c , however, the lesser variability of β_{140} is essential (as compared to the attenuation) at depth under 50 m. Many stations are characterized by constant values of β_{140} at deeper than 100 m depth (within the limits of measurement errors), although the attenuation goes on to fall with the depth.

2. Relations between hydro-optical parameters

In accordance with widely used model of formation of optical water parameters^{1,5} the index of the directed scattering is determined by three main fractions: natural water β^W ; fine, predominantly mineral hydrosol fraction β^S , and the fraction of coarse organic particles β^L . As a result, the values of b_B and β_{140} are expressed as

$$\begin{aligned} b_B &= 0.5b^W + B^S b^S + B^L b^L; \\ \beta_{140} &= \beta_{140}^W + g_{140}^S b^S + g_{140}^L b^L, \end{aligned} \quad (1)$$

where b^S, b^L are the values of scattering indices of individual fractions. According to Ref. 5, at $\lambda = 532 \text{ nm}$, $b^W = 0.0017 \text{ m}^{-1}$, $\beta_{140}^W = 1.6 \cdot 10^{-4} \text{ m}^{-1} \cdot \text{sr}^{-1}$, and the values of $B^{S,L}$ and $g_{140}^{S,L}$ are the following:

$B^S = 0.039$, $B^L = 6.4 \cdot 10^{-4}$, $g_{140}^S = 5.5 \cdot 10^{-3}$, $g_{140}^L = 6.05 \cdot 10^{-5}$. Since B^S is higher than B^L almost by two orders of magnitude, the value of backscattering in waters of different types is determined mainly by the concentration of fine mineral fraction.^{1,16}

Two main types of dependences between total scattering and backscattering were distinguished¹¹, based on the analysis of 869 measured scattering phase functions in different regions (including the data by V.I. Mankovsky for Lake Baikal¹⁷). The first type (W1) consists of the typical ocean waters, for which

$$\begin{aligned} b_B &= 0.5b^W + 0.00618(b - b^W) + 0.0032(b - b^W)^2, \\ 0.008 &< b < 9.3 \text{ m}^{-1}. \end{aligned} \quad (2)$$

To the second type (W2) the biological stable waters are referred, in which the content of mineral particles is less and the phytoplankton prevails:

$$\begin{aligned} b_B &= 0.5b^W + 0.00579 + 0.00462(b - b^W), \\ 0.09 &< b < 2.6 \text{ m}^{-1}. \end{aligned} \quad (3)$$

This dependence is characterized by the constant component in the backscattering, which does not depend on the scattering index variation and exceeds by several times the pure water backscattering.

This paper presents the measurement results of two parameters (c and β_{140}), not entering the relations (2), (3). First, the scattering index b should be estimated. Let us use the dependence,¹⁸ based on the analysis of experimental observations in ocean waters:

$$b = 0.944c - 0.048. \quad (4)$$

The dependence (4) takes into account both the minimal attenuation, determined by the actual absorption in the pure water ($a = 0.056 \text{ m}^{-1}$ at $\lambda = 550 \text{ nm}$),¹⁹ and the minimal albedo $\Lambda = b/c = 0.94$, observed in the extremely turbid coastal waters with $c = 20 \text{ m}^{-1}$ [Ref. 20]. In Baikal waters, the minimal absorption at depths between 200 and 400 m is observed at $\lambda = 490\text{--}510 \text{ nm}$ [Ref. 21] and at $\lambda = 532 \text{ nm}$ it is within the range $0.038\text{--}0.055 \text{ m}^{-1}$ [Ref. 22]. The independent measurement data on absorption and scattering indices in Baikal waters²³ confirm the validity of relation (4) for upper water layers.

With a knowledge of the scattering index and the measured value of β_{140} calculated by Eq. (4), it is possible to calculate the backscattering ratio, which is determined as $A_{140} = b/\beta_{140}$. Similar parameter is commonly used in laser sensing (lidar ratio

$A_{\pi} = b/\beta_{\pi}$). Figures 3 and 4 present both observation results and model dependences (1)–(3) in the coordinates (c, A_{140}) .

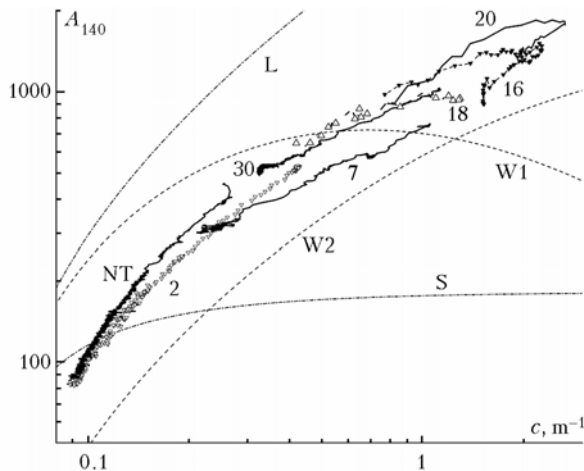


Fig. 3. Dependences of the A_{140} ratio for different monitoring stations.

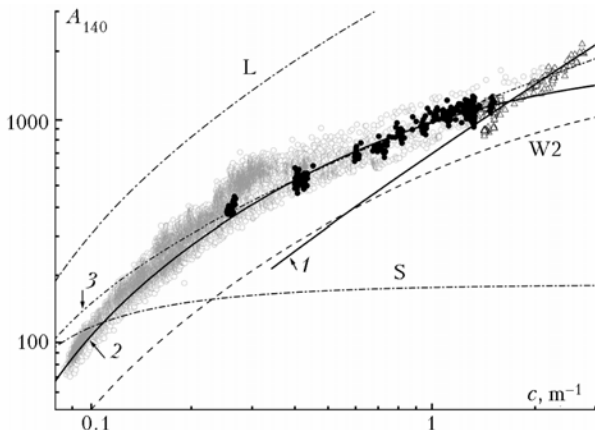


Fig. 4. Values of the backscattering ratio A_{140} in the upper 8-meter water layer in comparison with a total data series.

In the latter dependences, it is easily to pass to A_{140} using the above mentioned relation $b_B = \chi\beta_{140}$ at $\chi = 7.23$. In this case, the representation of diagrams in the coordinates (c, A_{140}) demonstrates more apparent than in the coordinates (b, b_B) the differences of the dependences for different types of water. The curves W1 and W2 in Fig. 3 correspond to the models (2) and (3). For the W2 type, the dependence $A_{140}(c)$ is monotonous, whereas for the W1 type, the maximum of A_{140} is observed at moderately high value of the attenuation index ($c \approx 0.8 \text{ m}^{-1}$). At a further growth of the water turbidity, the values of A_{140} decrease, that can be induced by the growth of the fine fraction content in water types, which were analyzed in Ref. 11. The curves L and S correspond to the dependences by the Kopelevich model (1) for the case, when all hydrosol is represented only by the coarse or fine fraction, respectively.

The numbers of the experimentally obtained dependences in Fig. 3 correspond to the numbers of

monitoring stations. For stations with profiles of the first type (NT, 2, and 30 in Fig. 3), the dependences of $A_{140}(c)$ are monotonous. Slope of the curves somewhat differs for different stations, but, on the whole, is close to the slope for the W2 type. A part of dependences for the stations of the second type (with attenuation maximum $h_{\max} \approx 8\div 10 \text{ m}$) is also characterized by the similar monotonous dependence. Figure 3 shows the dependence for station 7 and in Fig. 1 such stations are referred to the type 2a. The attenuation values for these stations do not exceed 1.6 m^{-1} (station 11). Other stations with more turbid water (from $c = 1.47 \text{ m}^{-1}$ for station 12 to $c = 2.7 \text{ m}^{-1}$ for station 17) have a typical ambiguity of the dependence in the near-surface layer. These stations are separated into type 2b; stations 16 and 20 are presented in Fig. 3.

The maximal value of A_{140} is observed at the depth h_{\max} , but the behaviors of the dependence higher and lower the maximum are different. Directly lower h_{\max} (between 2 and 3 m), A_{140} is constant, and then its behavior is similar to the dependence for stations of types 1 and 2a. However, when approaching the surface from the h_{\max} level, the dependence inclination for $A_{140}(c)$ is more abrupt, and values of A_{140} are essentially less, than for the same attenuation values lower h_{\max} . The intermediate dependence between types 1 and 2b was observed at station 18, where the maximum in distribution $c(h)$ is absent, but values of A_{140} near the surface are constant. Possibly, this is an intermediate state of the suspension vertical distribution, preceding the formation of the undersurface turbidity maximum.

In many cases (for instance, in interpretation of lidar data, when the sensing depth does not exceed 10 m in turbid waters), the relations of optical parameters are of a special interest just in the surface water layers. Figure 4 presents the dependences $A_{140}(c)$ in the upper 8-meter water layer for the depth profiles of types 1 and 2a (black circles) and 2b (triangles). Grey circles present the total data series for all stations. As it was mentioned, for water of the 2b type, the upper layer is described by a more abrupt dependence than for the W2 model, which can be characterized in the coordinates (b, b_B) by the relation

$$b_B = 0.5b^W + 0.008 + 0.00006(b - b^W) \quad (5)$$

(curve 1 in Fig. 4), which has the magnitude of the backscattering constant part close to the W2 type, but significantly lesser value of the backscattering probability for the variable hydrosol fraction, which coincides with that for the L model of large organic particles (1). This points to the fact that the increase of attenuation, when immersing from the surface to h_{\max} , proceeds at the expense of increasing content of large organic particles, which is concentrated in the region of the turbidity maximum. The dependence behavior of $A_{140}(c)$ for stations of 1 and 2a types almost coincides with the dependence for the total data series and can be expressed by the relation (curve 2 in Fig. 4)

$$b_B = 0.5b^W + 0.002 + 0.004(b - b^W). \quad (6)$$

In this case, the differences from W2 in the value of the backscattering constant part are significant. As in the dependence (3) for waters of the W2 type, in the obtained dependences (5) and (6) as the attenuation decreases with depth, b_B does not tend to $0.5b^W$ for the pure water. This means that in the deepest water layers, there is a slightly depth-varying (or even constant) fine hydrosol fraction with a higher backscattering index, than that for pure water.

At the same time, as follows from Fig. 4, the dependence $A_{140}(c)$ for the closest to the surface layer ($h < 0.5$ m) at all monitoring stations can be also interpreted by the curve 3, passing through the point ($c \approx 0.04$, $A_{140} = 10.6$) for pure water. It corresponds to the Kopelevich model (1) for the case when the ratio between fine and coarse fractions varies as the scattering index decreases, and is expressed by the approximate dependence $s = 0.15/(\sqrt{b} + 0.01)$, where s is the relative share of the fine fraction. And, correspondingly

$$\beta_{140} = \beta_{140}^W + [0.0055s + 0.0000605(1 - s)](b - b^W). \quad (7)$$

All the obtained dependences (5)–(7) confirm the apparent fact of increasing share of the fine fraction in clear waters.

Conclusions

The relations between the attenuation and backscattering indices are obtained, which are typical for the upper 300-meter layer of Baikal water. However, the ambiguity of near-surface layer complicates the adoption of some definite model. For the problems connected with observation of suspension spatial distribution near the surface, the use of relation (7) is more natural. For the problems of laser sensing, it is important to know the variation of lidar ratio with the depth, and in this case, one should choose among relations (5) and (6), taking into account the estimates of absolute value of the attenuation index in the sensing region.

The Kopelevich model (1) assumes that the angular distribution of the scattered radiation can be explained by the presence of only two hydrosol fractions, i.e., large organic and small mineral particles. Actually, the hydrosol content is more complicated. For instance, it is undoubtedly that a significant role in optical properties of Baikal water is played by small (micrometer) picoplankton.²⁴ In backscattering, the determining role is played by the index of refraction of the particle material,¹ which is *a priori* unknown. Therefore, interpretation of dependences given in this work can be only qualitative. The constancy of β_{140} (within the limits of measurement errors) under 100 m points out to the fine fraction predominance in backscattering, whose concentration is slightly variable. The relation (7) also points to the increase in a share of fine fraction

in more clear waters. The high value of the ratio A_{140} near the turbidity maximum speaks for the concentration of large organic particles in this layer. An abrupt inclination of the dependence $A_{140}(c)$ in the near-surface layer above the maximum points out that the backscattering variability is determined by a large fraction variability, although the absolute value of the backscattering probability is there higher than in the layer below maximum. Variations of A_{140} magnitude in local layers with the increased turbidity can be used for the qualitative diagnostics of the type of particles forming this layer.

References:

1. K.S. Shifrin, *Introduction to Oceanic Optics* (Gidrometeoizdat, Leningrad, 1983), 278 pp.
2. O.V. Kopelevich, in: *Opt. Oceana 1, Fiz. Opt. Oceana* (Nauka, Moscow, 1983), pp. 166–208.
3. N. Erlov, *Optical Oceanographic* (Mir, Moscow, 1970), 224 pp.
4. A.P. Ivanov, *Hydro-optical Foundations* (Nauka i Tekhnika, Minsk, 1975), 504 pp.
5. O.V. Kopelevich, in: *Opt. Oceana 1, Fiz. Opt. Oceana* (Nauka, Moscow, 1983), pp. 208–235.
6. V.I. Haltrin, *Appl. Opt.* **38**, 6826–6832 (1999).
7. K.J. Voss, *Limnol. Oceanogr.* **37**, No. 3, 501–509 (1992).
8. H.R. Gordon, O.B. Brown, R.H. Evans, et al., *J. Geophys. Res.* **93**, 10909–10924 (1988).
9. A.H. Barnard, W.S. Pegau, J.R.V. Zaneveld, *J. Geophys. Res. C* **3**, No. 11, 24955–24968 (1998).
10. R.A. Maffione and D.R. Dana, *Appl. Opt.* **36**, 6057–6067 (1997).
11. V.I. Haltrin, M.E. Lee, V.I. Mankovsky, et al., in: *Proc. of D. S. Rozhdestvensky Optical Society*, St. Petersburg (2003), pp. 252–257.
12. *c-beta Optical Attenuation and Backscattering Instrument. User's Manual*. HOBILabs Inc., Moss Landing, USA (2001), www.hobilabs.com.
13. P.P. Sherstyankin, G.P. Kokhanenko, I.E. Penner, et al., *Dokl. Ross. Akad. Nauk*, **383**, No. 1, 106–110 (2002).
14. *Baikal: Atlas* (Roskartografiya, Moscow, 2003), 65 pp.
15. P.P. Sherstyankin, in: *Physical Limnology of Lake Baikal: A Review* (Irkutsk; Okayama, 1994) pp. 24–30.
16. D. Stramsky and C.D. Mobley, *Limnol. Oceanogr.* **4**, 538–549 (1997).
17. V.I. Mankovsky and V.I. Haltrin, in: *Proc. of IEEE Int. Geosci. and Remote Sens. Symp. and 24th Canadian Symp. on Remote Sens.*, IEEE, Toronto, Canada (2002).
18. I.M. Levin and O.V. Kopelevich, in: *Proc. of D.S. Rozhdestvensky Optical Society*, St. Petersburg (2003), pp. 289–292.
19. R.M. Pope and E.S. Fry, *Appl. Opt.* **36**, No. 33, 8710–8722 (1997).
20. M. Sydor and R.A. Arnone, *Appl. Opt.* **36**, No. 27, 6905–6912 (1997).
21. P.P. Sherstyankin, *Experimental Investigations of Subglacial Field of Lake Baikal* (Nauka, Moscow, 1975), 90 pp.
22. G.P. Kokhanenko, B.A. Tarashchansky, N.M. Budnev, et al., *Proc. SPIE* **6160**, 2301–2312 (2005).
23. N.M. Budnev, G.P. Kokhanenko, M.M. Krekova, et al., *Atmos. Oceanic Opt.* **18**, Nos. 1–2, 96–104 (2005).
24. O.I. Belykh, T.G. Potemkina, N.G. Granin, et al., in: *Abstracts of Reports at the 4th Vereshchaginsk Baikal Conference* (Institute of Geography SB RAS, 2005), pp. 21–22.